Available online at www.sciencedirect.com

SciVerse ScienceDirect

Ceramics International 38 (2012) 3251–3260

CERAMICS INTERNATIONAL

www.elsevier.com/locate/ceramint

Processing and characterization of sol–gel titania membranes

Lecino Caldeira [a], Daniela C.L. Vasconcelos [a], Eduardo H.M. Nunes [a], Vilma C. Costa [a], Ana P. Musse [b], Sueli A. Hatimondi [b], Jaílton F. Nascimento [b], Wilson Grava [b], Wander L. Vasconcelos [a,*]

[a] *Department of Metallurgical and Materials Engineering, Federal University of Minas Gerais, Avenida Presidente Antônio Carlos, 6627, Campus da UFMG, Belo Horizonte, MG, CEP: 31270-901, Escola de Engenharia, bloco 2, sala 2230, Brazil*

[b] *Petrobras/CENPES, Avenida Horácio Macedo 950, Cidade Universitária, Ilha do Fundão, Rio de Janeiro, RJ, CEP: 21941-915, Brazil*

Received 8 November 2011; received in revised form 13 December 2011; accepted 14 December 2011
Available online 22 December 2011

Abstract

In this work we present a structural characterization of sol–gel titania membranes obtained in both supported and unsupported forms. We used two commercial grade alumina supports obtained from *Whatman* and *Rojan Advanced Ceramics*. The unsupported membranes were characterized by Fourier transform infrared spectroscopy (FTIR), thermogravimetric analysis (TG), differential scanning calorimetry (DSC), nitrogen sorption, and X-ray powder diffraction (XRD). Morphological studies were performed in both supported and unsupported membranes using a field emission scanning electron microscope (FE-SEM). In order to evaluate the performance of the supported membranes, single-gas permeation experiments were carried out at room temperature with nitrogen, helium, and carbon dioxide. We concluded from nitrogen sorption experiments that increasing the membrane heat treatment temperature leads to samples with lower specific surface areas and greater pore sizes. Close packed titania particles of uniform size were observed in SEM micrographs of unsupported membranes. The SEM analyses also revealed the presence of titania coatings on supported membranes. Some of the obtained membranes showed a separation capacity for He/CO_2 and He/N_2 larger than that expected for the Knudsen mechanism in the investigated pressure range. However, a good part of the analyzed samples showed an improvement of their separation capacity with increasing the feed pressure.
© 2012 Elsevier Ltd and Techna Group S.r.l. All rights reserved.

Keywords: E. Membrane; Sol–gel; Titania; Support; Dip-coating; Gas permeation

1. Introduction

Mass transport phenomena in porous materials have been investigated by several researchers over the last decades [1–3]. However, the precise characterization of this process is only achieved when materials with relatively simple pore structures are permeated by single gases or water. According to Burggraaf [4], the transport of gas mixtures is quite complex, especially in membrane systems with a complex pore architecture and operating at large pressure gradients. It is well established that several structural parameters including porosity, pore tortuosity, surface area, and pore diameter influence the mass transport in porous solids.

Mulder [5] defined ‘‘membrane’’ as a selective barrier between two phases. Its main function is to restrict totally or partially the transport of chemical species that compose these phases. According to Van de Water and Maschmeye [6], the membrane separation process presents advantages such as its relative simplicity, ease of use, low energy consumption, and application in the separation of both liquid and gas mixtures. In addition, it is possible to obtain membranes with tailored structures by using different materials including metals, polymers, and ceramics [7]. Although there are various commercially available methods for the separation and capture of gas species such as CO_2 and H_2, they are energy expensive and in some cases environmentally unfriendly [8]. For these reasons, the membrane technology has achieved in the last years a strategic importance.

The classification of membranes is very wide, it being possible to group them according to their origin (naturals and

* Corresponding author. Tel.: +55 31 3409 1821.
E-mail address: wlv@demet.ufmg.br (W.L. Vasconcelos).

0272-8842/$36.00 © 2012 Elsevier Ltd and Techna Group S.r.l. All rights reserved.
doi:10.1016/j.ceramint.2011.12.031

synthetics), nature (organic, inorganic, and hybrids), permeability (permeable, semi permeable, and impermeable), porosity (dense and porous), and pore size distribution (micro-, meso-, and macroporous). Organic membranes have been extensively used for industrial applications since the 1970s. They usually consist on a non-porous layer of 0.1–0.5 μm thickness, supported by a substrate with tailored porosity [9]. The incorporation of polymer chains into their structures is common [10–15]. However, organic membranes do not work well in harsh environments, in particular under chemical or thermal aggression [16].

Inorganic oxide membranes have been developed over the last fifty years primarily for the separation of uranium isotopes during its enrichment. However, in the 1980s, the advantages of chemically inert ceramic membranes with well-defined pore structures encouraged the investigation on gas separation properties and applications of inorganic membranes [16]. They usually consist of a macroporous support with successive thin layers deposited on it. The support must provide sufficient mechanical strength to prevent the membrane unit failure under the operating conditions. Intermediate layers bridge the gap between the large pores of the support and the small ones of the top layer. It is important to mention that only the top layer has separating capacities [17]. Inorganic membranes can be exposed to chemical surface modification processes and cleaning procedures which organic membranes do not withstand. These processes allow regenerating these materials, making them economically attractive.

Nanostructured titania membranes have received great attention over the last years because of their unique properties such as high water flux, semiconductance, and chemical stability [18,19]. Potential applications of titania membranes include ultrafiltration processes and catalytic/photocatalytic membrane reactor systems [20–22]. Titanium dioxide, particularly when in anatase form, is a photocatalyst under ultraviolet (UV) light. It is also well established that titanium dioxide, when doped with metal oxides like WO_3, is a photocatalyst under either visible or UV light. Due to these properties, titania has potential use in energy production because it can carry out hydrolysis to generate hydrogen for fuel cells and produce electricity when in nanoparticle form.

Houmard et al. [23] deposited both pure TiO_2 and hybrid organic–inorganic titanate–silicate thin films on silicon wafers via a sol–gel route. They observed that the wettability behavior of the prepared films depends on the amount of alkyl chains present in coatings framework. Vasconcelos et al. [24] monitored the structural evolution of sol–gel titania films deposited on 316L stainless steel substrates. They noticed the formation of a dimeric complex in a bidentate bridging coordination between the titanium isopropoxide and acetic acid. According to the film processing conditions, titanium atoms can also be present as pentacoordinated. Vasconcelos et al. [25] reported an increase of the corrosion resistance of stainless steel samples coated with sol–gel titania films.

In this work we present a structural characterization of sol–gel titania membranes obtained in both supported and unsupported forms. Two commercial grade alumina supports were used. They were obtained from *Rojan Advanced Ceramics* and *Whatman* (Anodisc). We have chosen these two alumina supports because they have different pore structures. The obtained asymmetric membranes are intended to be eventually used in gas separation processes. The coatings were prepared by sol–gel process. By using this chemical route, one can obtain ceramic materials with tailored properties, including composition, mechanical strength, and porosity. Another convenient feature of this technology is the fact that sol–gel samples can be obtained as bulks, thin films, and powders [26,27]. We used polyethylene glycol (PEG) as templating agent in coatings preparation because it allows obtaining sol–gel films with enhanced surface areas [28]. According to Fuertes and Soler-Illia [29], the combination of sol–gel processing with a controlled phase separation induced by polymers such as PEG or polypeptides is a simple strategy to produce oxide films with tailored porosities.

2. Experimental

In this work a new methodology for the synthesis of sol–gel titania was used. Initially a solution of nitric acid (HNO_3 – 65% – Aldrich) and absolute isopropanol (C_3H_7OH – Aldrich) was prepared. Under strong stirring, titanium isopropoxide (TIP – Aldrich) was slowly added to prevent the formation of precipitates. PEG was added to the sol after its previous dissolution in absolute isopropanol. The molar ratio TIP:-C_3H_7OH:HNO_3 was adjusted to 1:4:0.1.

Aliquots of the obtained solution were used in the synthesis of both supported and unsupported membranes. The unsupported membranes were prepared by pouring the sol in a 10 cm diameter Petri dish and drying it in a stove at 100 °C for 24 h. Supported membranes were obtained by dipping alumina supports in the sol and withdrawing them at a speed of 1.3 mm/min. As mentioned before, two different types of alumina supports were used. They were obtained from *Rojan Advanced Ceramics* and *Whatman* (Anodisc). Both supported and unsupported membranes were heated at 180 °C, 400 °C, 550 °C and 800 °C for 2 h. It is worth to mention that supported membranes prepared by using the *Whatman* support were not heat treated at 400 °C, 550 °C, and 800 °C because a maximum service temperature of about 400 °C is reported by the manufacturer in the material safety data sheet. In addition, permeability results of the supported membrane obtained by using the *Rojan* support and heat treated at 180 °C are not shown in this work because this material did not present a satisfactory separation capacity under the used experimental conditions. In order to facilitate the reader's understanding and keep a short notation, we have labeled the different alumina support/titania coating composites as follows:

- *Rojan* support/TiO_2 film: membrane R;
- *Whatman* support/TiO_2 film: membrane W.

The unsupported membranes were characterized by Fourier transform infrared spectroscopy (FTIR), thermogravimetric analysis (TG), differential scanning calorimetry (DSC),

nitrogen sorption, and X-ray powder diffraction (XRD). DSC and TG curves were obtained using DSC-50 and TG-50 Shimadzu apparatus, in the temperature ranges of 40–1000 °C and 40–500 °C respectively. Both DSC and TG analyses were performed using a heating rate of 10 °C/min and under nitrogen atmosphere (20 mL/min). XRD analyses were carried out in a Philips-PANalytical PW17-10 diffractometer, using Cu Kα radiation and operating at 40 kV and 30 mA. The diffractograms were recorded in the range of 10–90°, at a scan velocity of 0.06°/min. The identification of crystalline phases was performed by using JCPDS files numbers 21-1272 and 21-1276 for anatase and rutile phases, respectively. FTIR samples were prepared as pellets with KBr and analyzed in a Perkin-Elmer Paragon 1000. All spectra were recorded in the range from 4000 cm^{-1} to 300 cm^{-1}, with a resolution of 4 cm^{-1} and 128 scans. Nitrogen sorption experiments were performed in a Micromeritcs ASAP 2020, using samples preheated at 130 °C for until 48 h under vacuum. The specific surface areas of the analyzed samples were evaluated by using the BET multipoint method. Morphological studies were performed in both supported and unsupported membranes using a FEI QUANTA 200F field emission scanning electron microscope (FESEM). Compositional analyses were carried out with an EDS system (EDAX – Pegasus Microanalyzer) available in the SEM equipment.

In order to evaluate the membranes performance, single-gas permeation experiments were performed at room temperature with nitrogen, helium, and carbon dioxide. Disc shaped membranes were placed in a Wicke–Kallenbach type cell made of stainless steel. The gas flow through the membrane was measured with a soap film flow meter. The pressure difference across the membranes was measured with a MKS Baratron pressure transducer model 627B. Before each permeability experiment the leak-free system was evacuated with an Edwards two stage vacuum pump model E2M2. A schematic representation of the gas permeation apparatus used is shown elsewhere [30].

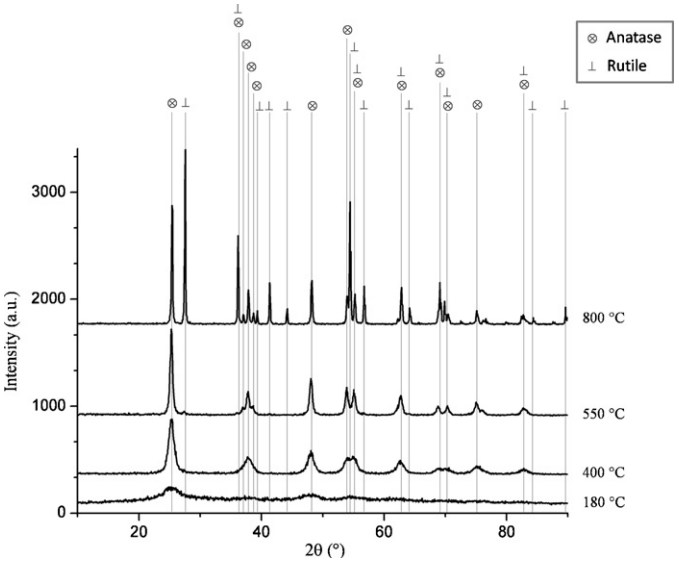

Fig. 1. XRD patterns of unsupported membranes.

3. Results and discussion

Fig. 1 shows XRD patterns of unsupported membranes prepared in this work. One observes that the higher the heat treatment, the more intense are the XRD peaks ascribed to rutile. This observation matches with the expected phase transformation from anatase to rutile in the investigated temperature range. According to Carp et al. [31], the enthalpy associated to the anatase–rutile phase transformation is relatively low, ranging from -1.3 to -6.0 ± 0.8 kJ/mol. However, at room temperature the kinetics of this phase transformation is so slow that it practically does not occur. At macroscopic scale this transformation reaches a measurable kinetics at temperatures above 600 °C [32].

Fig. 2(a) and (b) shows TG and DSC curves obtained for unsupported membranes. The sample heat treated at 180 °C showed the higher mass loss among the analyzed membranes. We observed three main events of mass loss in the TG curve of this sample. The first one, located around 100 °C, is associated to the removal of organic residues and water from the porous gel network. The sharp decrease in weight around 300 °C seems to be related to the removal of hydroxyl groups. The last event of mass loss at 600 °C is ascribed to the removal of residual structural water and stabilizing anions [33,34].In the DSC curve the removal of organic residues and water from the titania network is related to a broad endothermic peak at 100 °C. The

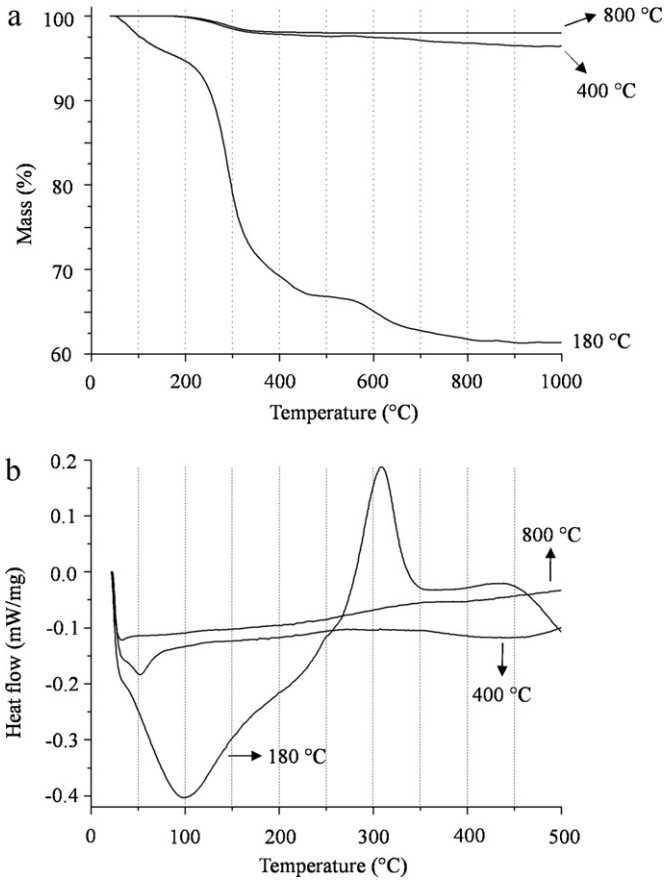

Fig. 2. (a) TG and (b) DSC curves of unsupported membranes heat treated at 180 °C, 400 °C, and 800 °C.

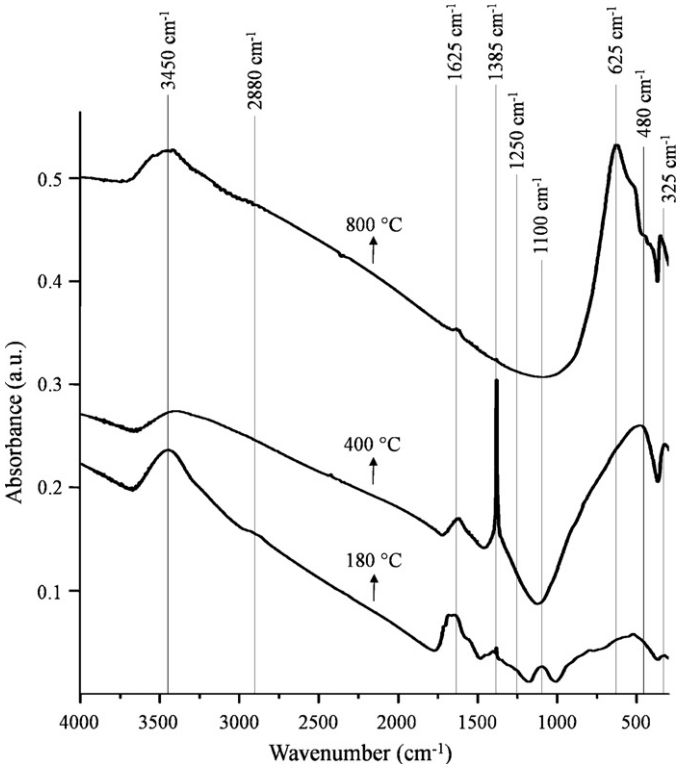

Fig. 3. FTIR spectra of unsupported membranes heat treated at 180 °C, 400 °C, and 800 °C.

sample treated at 180 °C presented the sharpest peak among the unsupported membranes. This observation matches with the greater mass loss shown by this material at this temperature range in TG analyses. The exothermic peak around 300 °C is associated to the titania gel crystallization [33]. In fact, XRD experiments revealed that samples heat treated at 400 °C and 800 °C presented greater crystallinity than that heated at 180 °C.

Fig. 3 shows FTIR spectra of unsupported membranes heated at 180 °C, 400 °C and 800 °C. The bands at 325 cm^{-1}, 480 cm^{-1}, and 625 cm^{-1}, which are characteristic of the infrared spectrum of titania, are ascribed to Ti–O and Ti–O–Ti bonds. The band at 1385 cm^{-1} is caused by the symmetric deformation mode of CH_3 groups from the isopropoxide structure [35,36]. The peak located at 1625 cm^{-1} is associated to the symmetric vibration mode of carbonyl groups. The broad band centered at about 3450 cm^{-1} is related to molecular water and hydroxyls [37–39].

We observed three additional peaks at 1100 cm^{-1}, 1250 cm^{-1}, and 2880 cm^{-1} in the FTIR spectrum of the sample treated at 180 °C. These bands are ascribed to C–O–C and C–H bonds from polyethylene glycol [40]. The presence of these bands reveals that the heat treatment was not sufficient to promote PEG removal from the membrane. Matsuda [41] showed that during heat treatment in air PEG starts to decompose only around 250 °C and that a temperature of at

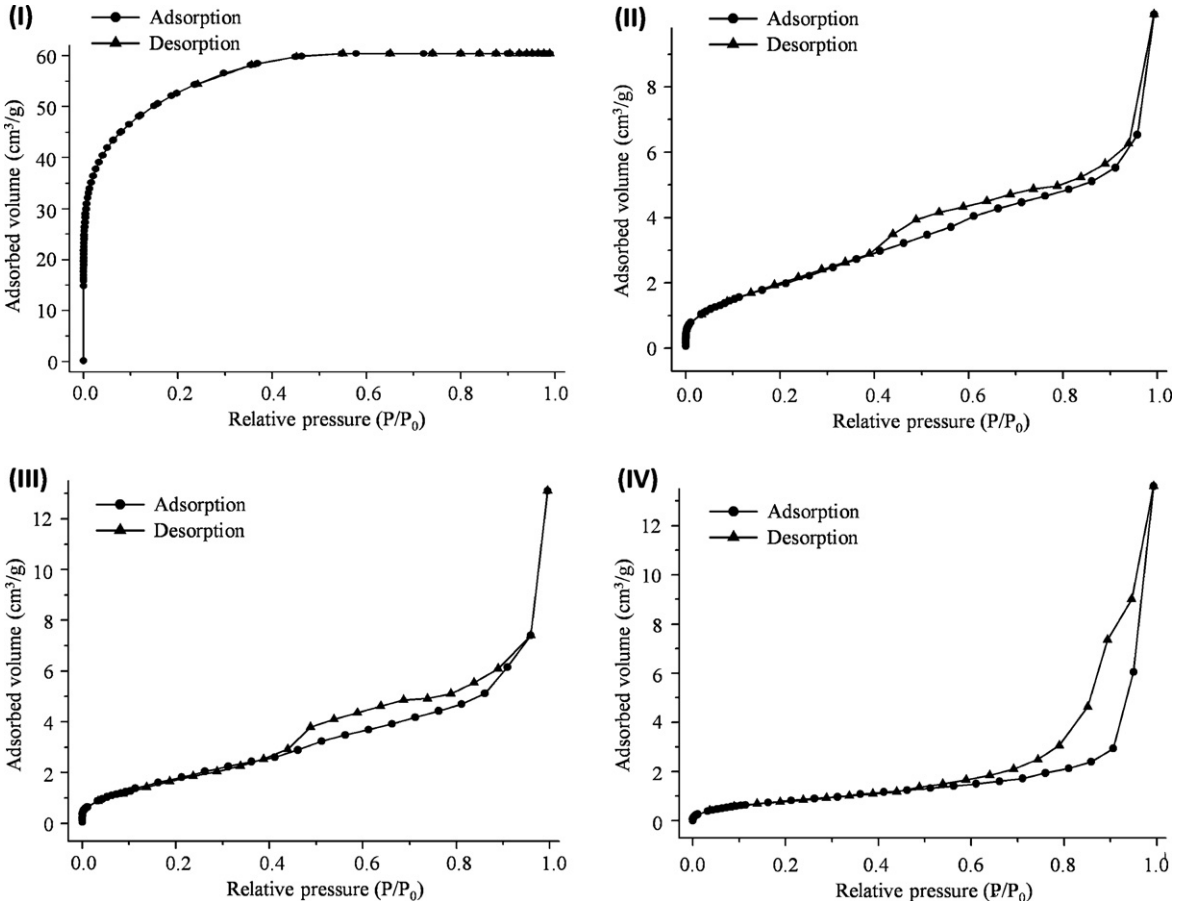

Fig. 4. Nitrogen sorption isotherms of unsupported membranes. Samples heat treated at (I) 180 °C, (II) 400 °C, (III) 550 °C, and (IV) 800 °C.

Table 1
Specific surface areas of unsupported membranes.

Heat treatment temperature (°C)	Specific surface area (m^2/g)
180	187
400	8
550	7
800	3

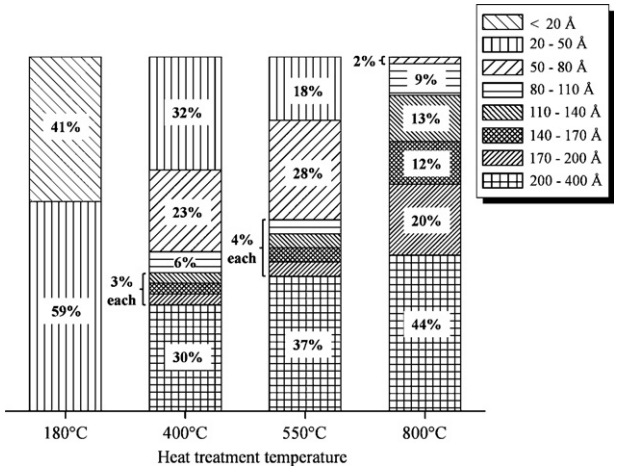

Fig. 5. Contribution of each pore size class to the porosity assessed by nitrogen.

least 300 °C is necessary to completely remove PEG from titania.

Fig. 4 shows nitrogen sorption isotherms of unsupported membranes. According to IUPAC [42], the sample treated at 180 °C exhibits a typical isotherm of microporous material, whereas the other ones present isotherms characteristic of mesoporous solids. As given in Table 1, increasing the membrane heat treatment temperature leads to materials with lower specific surface areas.

Fig. 5 presents the contribution of each pore size class to the porosity assessed by nitrogen sorption. This evaluation is based on cumulative pore volume curves obtained by applying the NLDFT method on the isotherms shown in Fig. 5. We observed that the higher the heat treatment temperature, the greater the pore size of the sample.

Fig. 6 exhibits typical micrographs of unsupported titania membranes obtained in this work. One observes that the TiO_2 particles are close packed with formation of necks among them. This observation reinforces that by using the sol–gel process it is possible to obtain materials with tailored porosity and mechanical strength, even at low processing temperatures. It is worth pointing out the size homogeneity of the particles.

Fig. 7 presents SEM micrographs of the membrane R. The presence of titania among the alumina particles is highlighted when the bulk of the substrate and film are compared. Fig. 8(a)

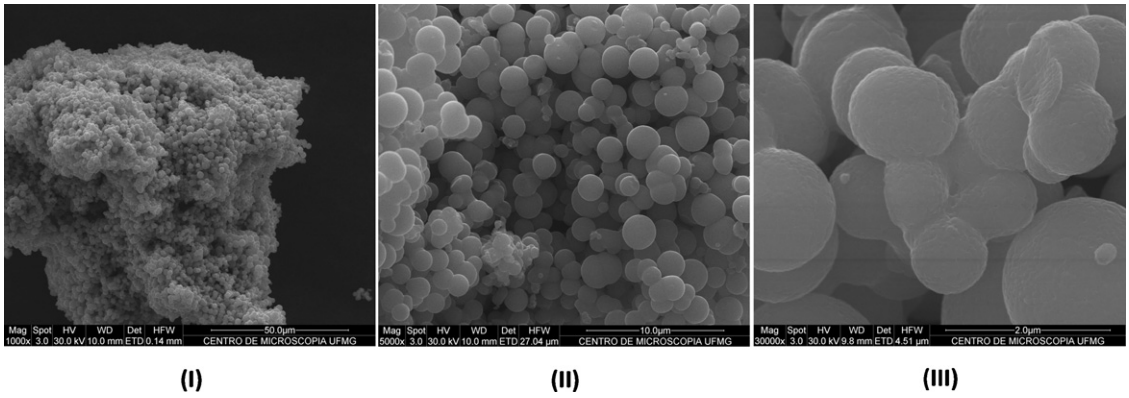

Fig. 6. Typical micrographs of unsupported titania membrane prepared in this work. The scale bars correspond to (I) 50 μm, (II) 10 μm, and (III) 2 μm.

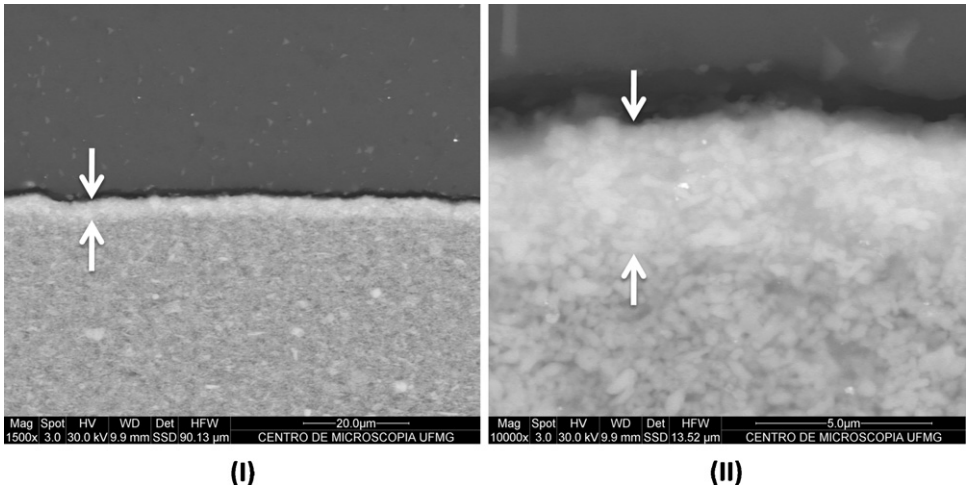

Fig. 7. SEM micrographs of the membrane R. Supported membrane heat treated at 180 °C. The scale bars correspond to (I) 20 μm and (II) 5 μm.

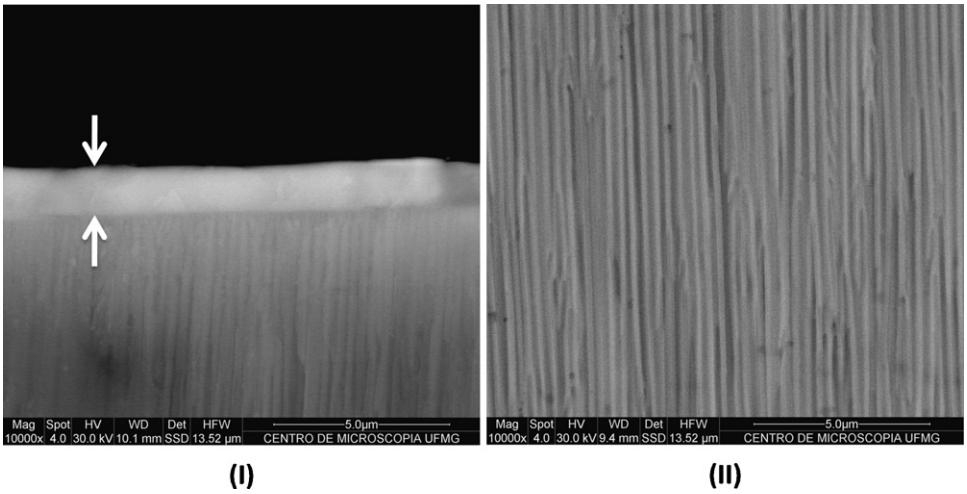

Fig. 8. SEM micrographs of the membrane W. Supported membrane heat treated at 180 °C. (a) Cross section of the membrane and (b) micrograph of the bulk of the substrate. The scale bars in both images represent 5 μm.

shows the cross section of the membrane W. We observed the presence of a defect-free coating of about 1 μm thickness. The presence of the titania film on both supports was also confirmed by EDS analyses. In Fig. 8(b) is shown a micrograph of the bulk area of the substrate. As observed by Smuleac et al. [43], the *Whatman* support is formed by an ordered array of straight channels. The distinct pore structures presented by these two alumina supports are related to the different processing methods used: *Rojan Ceramics* uses the extrusion process to obtain their supports, whereas *Whatman* applies an anodic oxidation method. Due to this the *Rojan* support exhibits a dispersed pore structure. According to Li et al. [44], the anodic oxidation process allows to obtain samples with a highly ordered pore array.

Fig. 9 presents the CO_2 permeance as a function of the feed pressure for the studied supports. The dotted lines are used only as guide to the eyes. Koros et al. [45] defined permeance as the ratio between the gas amount which flows through a plane of unit area per unit time, and the partial pressure difference across the membrane. We observed that the *Whatman* support showed a higher resistance to the gas flow than the *Rojan* one. Again, this difference arises from the distinct pore structural characteristics of both samples.

Fig. 10 shows the CO_2 permeance as a function of the feed pressure for the *Rojan* support, before and after the deposition of titania films on its surface. In general, increasing the membrane heating temperature resulted in decreasing the system permeance. DeHoff and Rhines [46] defined the genus as "the maximum number of non-self reentrant closed curves which may be constructed on the surface without dividing it into two separate parts". One can show that the genus of a closed surface is equal to the connectivity of the volume responsible for its origin. Assuming the presence of cylindrical pores, the genus per unit volume (G_V) of a given structure can

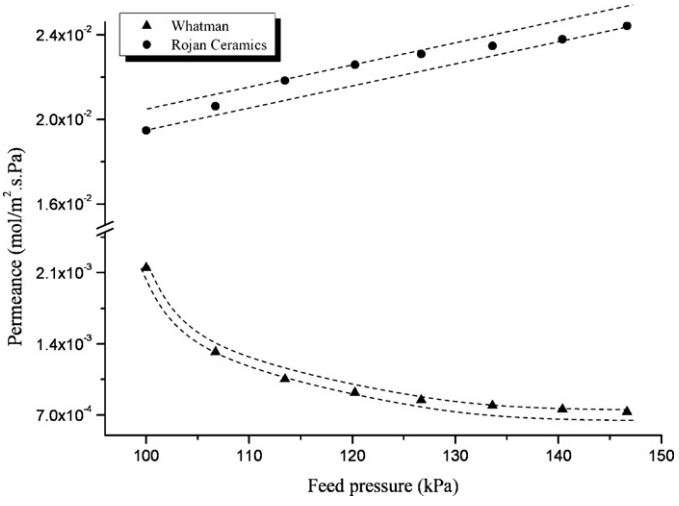

Fig. 9. CO_2 permeance as a function of the feed pressure for the studied supports.

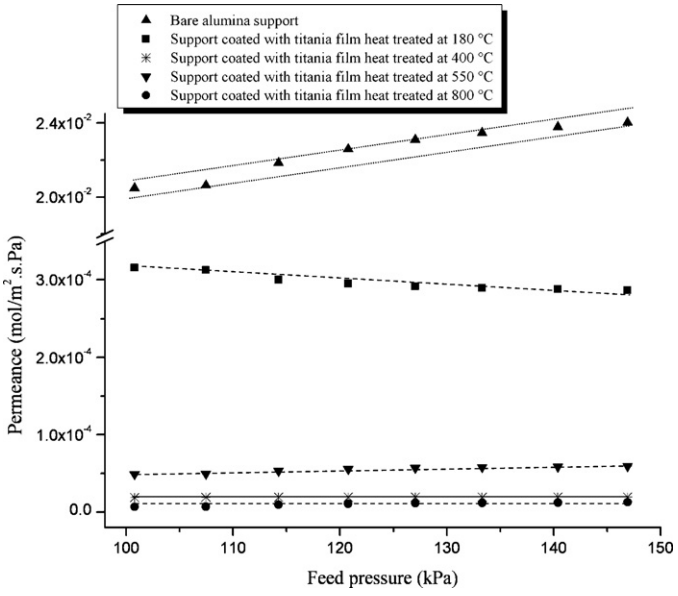

Fig. 10. CO_2 permeance as a function of the feed pressure for the *Rojan Ceramics* support, before and after the deposition of titania films heat treated at different temperatures on its surface.

Table 2
Genus per unit volume (G_V) evaluated for unsupported membranes.

Heat treatment temperature (°C)	G_V (cm^{-3})
180	2.1×10^{19}
400	9.2×10^{15}
550	5.5×10^{15}
800	4.0×10^{14}

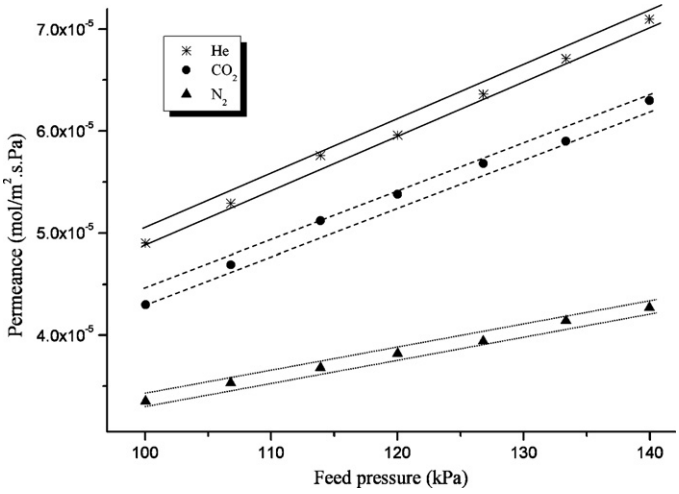

Fig. 11. Typical single gas permeances of He, N_2, and CO_2 through the membrane R.

be evaluated by [47]:

$$G_v = \frac{S_v^3}{16\pi V_v(1-V_v)}, \quad (1)$$

where S_V is the pore surface area per unit volume, and V_V the pore volume fraction. As given in Table 2, increasing the heat treatment temperature of titania leads to structures with lower connectivities. We believe that the observed decrease in titania permeability could be largely due to the decrease of its pore network connectivity. It deserves stress that the pore size range assessed by nitrogen sorption is typically below 400 Å. Thus, this hypothesis about the decrease of the pore network connectivity only applies to pores in this size range.

Fig. 11 shows the typical single gas permeances of He, N_2 and CO_2 through the membrane R. The dotted lines are only guides to the eyes. By comparing these curves, we have evaluated the separation factors for the He/CO_2, He/N_2, and N_2/CO_2 systems (see Fig. 12). Because of the similar kinetic diameter of nitrogen and carbon dioxide, the N_2/CO_2 system showed separation efficiency lower than those observed for the He/CO_2 and He/N_2 systems; since helium is smaller and lighter than CO_2 and N_2, it diffuses much faster through the membrane framework [48]. In general, the separation capacity decreased with increasing the membrane heat treatment temperature. As shown in Fig. 5, the higher the sample heating temperature, the greater is its pore size. This results in decreasing the separation capacity of the membrane. We also observed that for samples heated at 400 °C and 550 °C, increasing the feed pressure leads to improving its separation efficiency. This is an important result because the known high thermal and mechanical stabilities of the alumina/titania system are likely to allow its use in high pressure applications.

Fig. 13 shows the CO_2 permeance as a function of the feed pressure for the *Whatman* support, before and after the deposition of a titania film on its surface (the dotted lines are

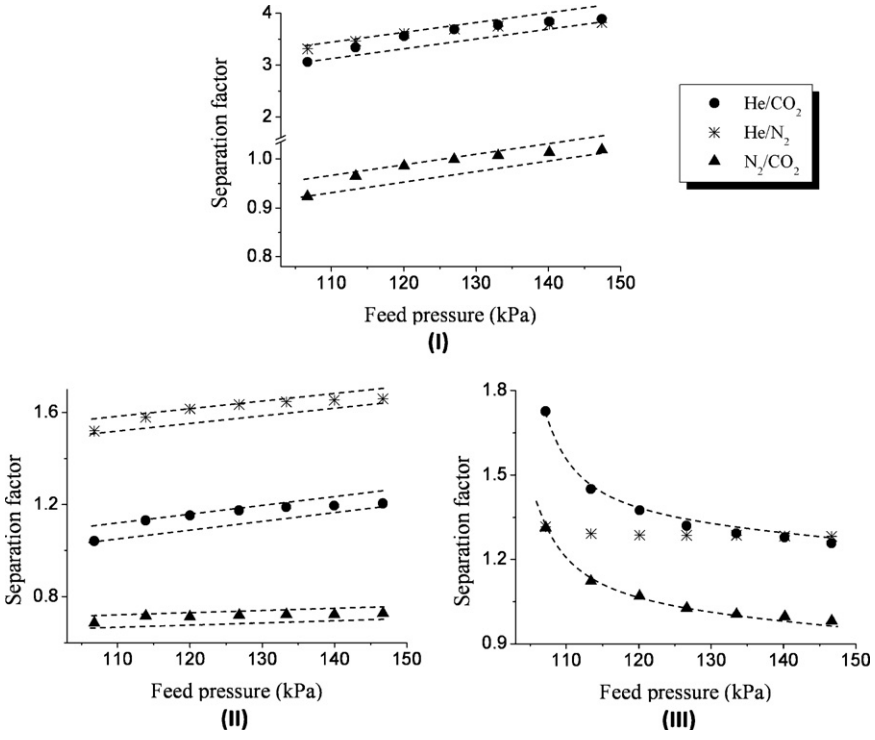

Fig. 12. Separation factors for He/CO_2, He/N_2, and N_2/CO_2 for the membrane R after heat treatment at (I) 400 °C, (II) 550 °C, and (III) 800 °C.

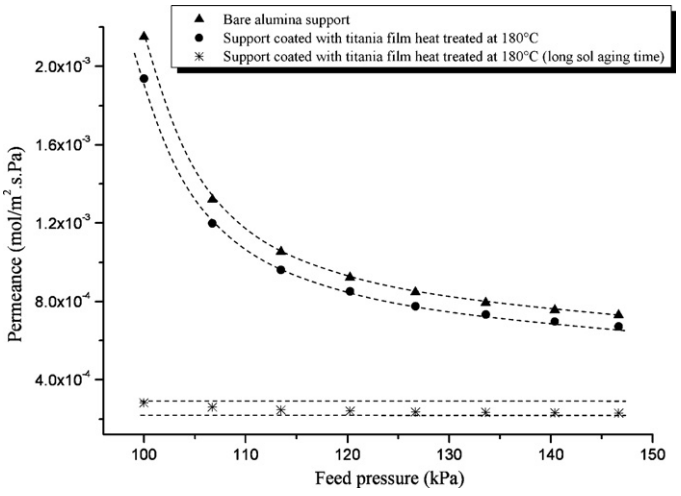

Fig. 13. CO_2 permeance as a function of the feed pressure for the *Whatman* support, before and after the deposition of a titania film heat treated at 180 °C.

only guides to the eyes). We observed that the presence of the TiO_2 coating has little influence on the permeance of the alumina support. However, this scenario changes when the sol aging time is increased. According to Wang and Hu [49], the titania film thickness increases with increasing the sol aging time, because the longer the aging time, the higher the sol viscosity. Based on these observations, we have chosen to perform the permeability tests in the membrane in which the titania film was derived from the sol aged for longer periods of time. Fig. 14 shows the permeability results obtained for this membrane (the dotted lines are only guides to the eyes). As observed for the membrane R, increasing the feed pressure leads to improving its separation efficiency.

Properties of gas flow in porous solids depend on the ratio of the number of molecule–molecule collisions to that of the molecule–wall collisions. When the number of intermolecular collisions is strongly dominant, the Poiseuille mechanism is

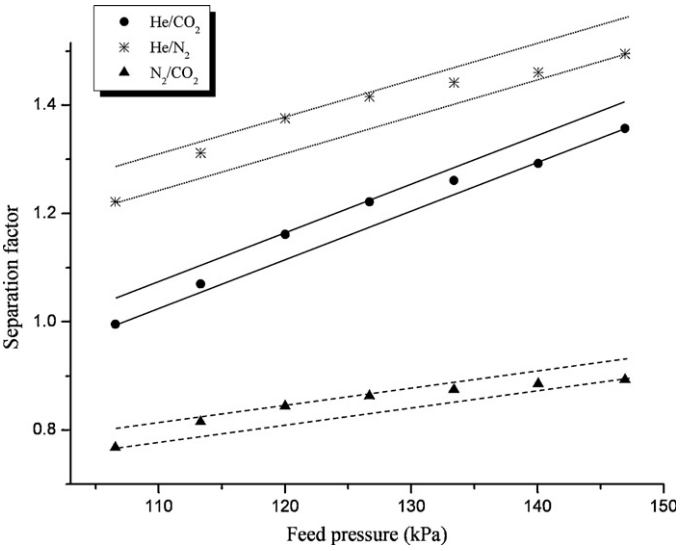

Fig. 14. Separation factors for He/CO_2, He/N_2, and N_2/CO_2 for the membrane W. Supported membrane obtained after a long sol aging time.

present. It is well established that for systems in which this mass transport mechanism is dominant, the permeance (F_V) of a given gas is described by:

$$F_V \propto \frac{P_m}{\eta}, \tag{2}$$

where P_m and η are the average pressure and dynamic viscosity of the gas. Based on this relation, we can conclude that at a given pressure:

$$F_V(He) < F_V(N_2) < F_V(CO_2). \tag{3}$$

This was not observed for the analyzed membranes. This suggests that the Poiseuille mechanism is not dominant in the studied membranes, and indicates the absence of large amounts of defects in them. However, the linear increase of the permeance with the feed pressure reveals that the Poiseuille mechanism may be contributing to the gas flow through the membrane.

When the number of molecule–wall collisions is strongly dominant, the flow of a single gas through a capillary under the action of a pressure gradient can be described by the Knudsen equation [4]:

$$F_{Kn} \propto \frac{1}{\sqrt{M}}, \tag{4}$$

where F_{Kn} and M are the permeance and molecular weight of the gas. Thus, for membranes in which the Knudsen regime is dominant, the permeance plotted versus the feed pressure should give rise to a horizontal line because F_{Kn} is pressure independent. Moreover, it can be shown from Eq. (5) that:

$$\frac{F_{Kn}(He)}{F_{Kn}(CO_2)} \approx 3.3, \tag{5}$$

$$\frac{F_{Kn}(He)}{F_{Kn}(N_2)} \approx 2.6, \tag{6}$$

$$\frac{F_{Kn}(N_2)}{F_{Kn}(CO_2)} \approx 1.3. \tag{7}$$

Among the studied systems, only the membrane R heat treated at 400 °C showed separation factor larger than the expected for the Knudsen mechanism in the investigated pressure range. However, we have to consider that increasing the feed pressure has resulted in improving the separation capacity of most of the analyzed membranes. As already discussed, it is an important result because the known high thermal and mechanical stabilities of the alumina/titania system is expected to allow its use in high pressure applications.

4. Conclusions

Thermal analyses revealed that the titania unsupported membranes started to crystallize at temperatures around 300 °C. XRD experiments showed that the higher the heat treatment temperature, the more intense are the XRD peaks ascribed to rutile. The presence of characteristic absorption bands from polyethylene glycol in the FTIR spectrum of the

unsupported membrane heated at 180 °C reveals that the heat treatment was not sufficient to promote the complete removal of PEG from titania. We concluded from nitrogen sorption experiments that increasing the membrane heat treatment temperature leads to samples with lower specific surface areas and greater pore sizes. Close packed titania particles of uniform size were observed in micrographs of unsupported membranes. SEM analyses also revealed the presence of titania coatings on supported membranes.

Among the studied supports, the obtained one from *Rojan Advanced Ceramic* presented better response to the titania film deposition, with a separation factor for the He/CO_2 and He/N_2 systems larger than that expected for the Knudsen mechanism in the investigated pressure range. Because of the similar kinetic diameter of nitrogen and carbon dioxide, the N_2/CO_2 system showed separation efficiency lower than those observed for the He/CO_2 and He/N_2 systems; since helium is smaller and lighter than CO_2 and N_2, it diffuses much faster through the membrane framework. We observed that increasing the membrane heat treatment temperature decreased the system permeance. Through a structural model we showed that increasing the titania heat treatment temperature leads to structures with lower connectivities. Among the processing parameters that must be better studied in future tests, it is worth to point out the deposition procedure of the titania coating, the heat treatment step, and the effect of intermediate layers between the substrate and the titania film on the system performance.

Acknowledgements

The authors thank Andrea Bicalho and the UFMG Microscopy Center for their technical support in the XRD and SEM analyses, respectively. We also thank CNPq, Fapemig, and Petrobras for the financial support of this research.

References

[1] R.E. Cunningham, R.J.J. Williams, Diffusion in Gases and Porous Media, 1st ed., Plenum Press, New York, 1980.
[2] J. Kärger, D.M. Ruthven, Diffusion in Zeolites and Other Microporous Solids, 1st ed., John Wiley & Sons, New York, 1992.
[3] J. Rouquerol, D. Avnir, C.W. Fairbridge, D.H. Everett, J.M. Haynes, N. Pernicone, J.D.F. Ramsay, K.S.W. Sing, K.K. Unger, Recommendations for the characterization of porous solids, Pure Appl. Chem. 66 (1994) 1739–1758.
[4] A.J. Burggraaf, Transport and separation properties of membranes with gases and vapours, in: A.J. Burggraaf, L. Cot (Eds.), Fundamentals of Inorganic Membrane Science and Technology, 1st ed., Elsevier, New York, 1996, pp. 331–433.
[5] M. Mulder, Basic Principles of Membrane Technology, 5th ed., Kluwer Academic Publishers, Dordrecht, 1996.
[6] L.G.A. Van de Water, T. Maschmeyer, Mesoporous membranes: a brief overview of recent developments, Top. Catal. 29 (2004) 67–77.
[7] E. Drioli, M. Romano, Progress and news perspectives on integrated membrane operations for sustainable industrial growth, Ind. Eng. Chem. Res. 40 (2001) 1277–1300.
[8] Y.T. Seo, S.P. Kang, H. Lee, C.S. Lee, W.M. Sung, Hydrate phase equilibria for gas mixtures containing carbon dioxide: a proof-of-concept to carbon dioxide recovery from multicomponent gas stream, Korean J. Chem. Eng. 17 (2000) 659–667.
[9] T. Bein, Synthesis and applications of molecular sieve layers and membranes, Chem. Mater. 8 (1996) 1636–1653.
[10] Y.F. Fu, S.W. Hsiao, C.C. Hu, H.Z. Qui, K.R. Lee, Effect of physical aging on sorption and permeation of small molecules in polyimide membranes, Desalination 234 (2008) 58–65.
[11] M. Mikawa, N. Seki, S. Nagaoka, H. Kawakami, Structure and gas permeability of asymmetric polyimide membranes made by dry-wet phase inversion: influence of alcohol as casting solution, J. Polym. Sci. Polym. Phys. 45 (2007) 2739–2746.
[12] A. Torres-Trueba, F.A. Ruiz-Trevino, G. Luna-Barcenas, C.H. Ortiz-Estrada, Formation of integrally skinned asymmetric polysulfone gas separation membranes by supercritical CO_2, J. Membr. Sci. 320 (2008) 431–435.
[13] M. Iqbal, Z. Man, H. Mukhtar, B.K. Dutta, Solvent effect on morphology and CO_2/CH_4 separation performance of asymmetric polycarbonate membranes, J. Membr. Sci. 318 (2008) 167–175.
[14] W.J. Koros, A.H. Chan, D.R. Paul, Sorption and transport of various gases in polycarbonate, J. Membr. Sci. 2 (1977) 165–190.
[15] J.M. Cheng, D.M. Wang, F.C. Lin, J.Y. Lai, Formation and gas flux of asymmetric PMMA membranes, J. Membr. Sci. 109 (1996) 93–107.
[16] J.C.D. da Costa, G.Q. Lu, H.Y. Zhu, V. Rudolph, Novel composite membranes for gas separation: preparation and performance, J. Porous Mater. 6 (1999) 143–151.
[17] P.M. Biesheuvel, H. Verweij, Design of ceramic membrane supports: permeability, tensile strength and stress, J. Membr. Sci. 156 (1999) 141–152.
[18] S.H. Hyun, B.S. Kang, Synthesis of titania composite membranes by the pressurized sol–gel technique, J. Am. Ceram. Soc. 79 (1996) 279–282.
[19] K.N.P. Kumar, K. Keizer, A.J. Burggraaf, T. Okubo, H. Nagamoto, Textural evolution and phase transformation in titania membranes: Part 2. Supported membranes, J. Mater. Chem. 3 (1993) 1151–1159.
[20] T. Tsuru, D. Hironaka, T. Yoshioka, M. Asaeda, Titania membranes for liquid phase separation: effect of surface charge on flux, Sep. Purif. Technol. 25 (2001) 307–314.
[21] A.L. Ahmad, M.R. Othman, H. Mukhtar, H2 separation from binary gas mixture using coated alumina–titania membrane by sol–gel technique at high-temperature region, Int. J. Hydrogen Energy 29 (2004) 817–828.
[22] J. Kim, J.W. Lee, T.G. Lee, S.W. Nam, J. Han, Nanostructured titania membranes with improved thermal stability, J. Mater. Sci. 40 (2005) 1797–1799.
[23] M. Houmard, D.C.L. Vasconcelos, W.L. Vasconcelos, G. Berthomé, J.C. Joud, M. Langlet, Water and oil wettability of hybrid organic–inorganic titanate–silicate thin films deposited via a sol–gel route, Surf. Sci. 603 (2009) 2698–2707.
[24] D.C.L. Vasconcelos, V.C. Costa, E.H.M. Nunes, A.C.S. Sabioni, M. Gasparon, W.L. Vasconcelos, Infrared spectroscopy of titania sol–gel coatings on 316L stainless steel, Mater. Sci. Appl. 2 (2011) 1375–1382.
[25] D.C.L. Vasconcelos, E.H.M. Nunes, A.C.S. Sabioni, J.C.D. da Costa, W.L. Vasconcelos, Structural characterization and corrosion behavior of stainless steel coated with sol–gel titania, J. Mater. Eng. Perform., doi:10.1007/s11665-011-9919-y, in press.
[26] A. Yasumori, H. Shinoda, Y. Kameshima, S. Hayashi, K. Okada, Photocatalytic and photoelectrochemical properties of TiO_2-based multiple layer thin film prepared by sol–gel and reactive-sputtering methods, J. Mater. Chem. 11 (2001) 1253–1257.
[27] L.L. Hench, W.L. Vasconcelos, Sol–gel silica science, Annu. Rev. Mater. Sci. 20 (1990) 269–298.
[28] M.C. Bautista, A. Morales, Silica antireflective films on glass produced by the sol–gel method, Sol. Energy Mater. Sol. Cells 80 (2003) 217–225.
[29] M.C. Fuertes, G.J.A.A. Soler-Illia, Processing of macroporous titania thin films: from multiscale functional porosity to nanocrystalline macroporous TiO_2, Chem. Mater. 18 (2006) 2109–2117.
[30] L.L.O. Silva, D.C.L. Vasconcelos, E.H.M. Nunes, L. Caldeira, V.C. Costa, S.A. Hatimondi, J.F. Nascimento, W. Grava, W. Vasconcelos, Processing, structural characterization and performance of alumina supports used in ceramic membranes, Ceram. Int., doi:10.1016/j.ceramint.2011.10.025, in press.

[31] O. Carp, C.L. Huisman, A. Reller, Photoinduced reactivity of titanium dioxide, Prog. Solid State Chem. 32 (2004) 33–177.
[32] W.W. So, S.B. Park, K.J. Kim, C.H. Shin, S.J. Moon, The crystalline phase stability of titania particles prepared at room temperature by the sol–gel method, J. Mater. Sci. 36 (2001) 4299–4305.
[33] K.N.P. Kumar, K. Keizer, A.J. Burggraaf, Textural evolution and phase transformation in titania membranes: Part 1. Unsupported membranes, J. Mater. Chem. 3 (1993) 1141–1149.
[34] S. Akbarnezhad, S.M. Mousavi, R. Sarhaddi, Sol–gel synthesis of alumina–titania ceramic membrane: preparation and characterization, Indian J. Sci. Technol. 3 (2010) 1048–1051.
[35] M. Burgos, M. Langlet, The sol–gel transformation of TIPT coatings: a FTIR study, Thin Solid Films 349 (1999) 19–23.
[36] D.P. Birnie, Esterification kinetics in titanium iso-propoxide–acetic acid solutions, J. Mater. Sci. 35 (2000) 367–374.
[37] D.L. Wood, E.M. Rabinovich, D.W. Johnson, J.B. MacChesney, E.M. Vogel, Preparation of high-silica glasses from colloidal gels. 3. Infrared spectrophotometric studies, J. Am. Ceram. Soc. 66 (1983) 693–699.
[38] Y. Djaoued, R. Brüning, D. Bersani, P.P. Lottici, S. Badilescu, Sol–gel nanocrystalline brookite-rich titania films, Mater. Lett. 58 (2004) 2618–2622.
[39] B. Siffert, J.F. Li, Determination of the fraction of bound segments of PEG polymers at the oxide–water interface by microcalorimetry, Colloids Surf. 40 (1989) 207–217.
[40] Y. Djaoued, J. Robichaud, R. Brüning, A.S. Albert, P.V. Ashrit, The effect of poly(ethylene glycol) on the crystallisation and phase transitions of nanocrystalline TiO_2 thin films, Mater. Sci.—Poland 23 (2005) 15–27.
[41] A. Matsuda, Y. Matsuno, S. Katayama, T. Tsuno, N. Tohge, T. Minami, Physical and chemical properties of titania–silica films derived from poly(ethyleneglycol)-containing gels, J. Am. Ceram. Soc. 73 (1990) 2217–2221.
[42] K.S.W. Sing, D.H. Everett, R.A.W. Haul, L. Moscou, R.A. Pierotti, J. Rouquérol, T. Siemieniewska, Reporting physisorption data for gas/solid systems with special reference to the determination of surface area and porosity, Pure Appl. Chem. 57 (1985) 603–619.
[43] V. Smuleac, D.A. Butterfield, S.K. Sikdar, R.S. Varma, D. Bhattacharyya, Polythiol-functionalized alumina membranes for mercury capture, J. Membr. Sci. 251 (2005) 169–178.
[44] A.P. Li, F. Muller, A. Birner, K. Nielsch, U. Gösele, Hexagonal pore arrays with a 50–420 nm interpore distance formed by self-organization in anodic alumina, J. Appl. Phys. 84 (1998) 6023–6026.
[45] W.J. Koros, Y.H. Ma, T. Shimidzu, Terminology for membranes and membrane processes, J. Membr. Sci. 120 (1996) 149–159.
[46] R.T. DeHoff, F.N. Rhines, Quantitative Microscopy, 1st ed., McGraw-Hill, New York, 1968.
[47] W.L. Vasconcelos, R.T. DeHoff, L.L. Hench, Structural evolution during sintering of optical sol–gel silica, J. Non-Cryst. Solids 121 (1990) 124–127.
[48] K. Kusakabe, T. Kuroda, S. Morooka, Separation of carbon dioxide from nitrogen using ion-exchanged faujasite-type zeolite membranes formed on porous support tubes, J. Membr. Sci. 148 (1998) 13–23.
[49] B. Wang, L. Hu, Effect of processing parameters on the optical properties of TiO_2/osmosil planar waveguide, J. Sol–Gel Sci. Technol. 34 (2005) 71–76.